Microbiological Research 280 (2024) 127600

Contents lists available at ScienceDirect

Microbiological Research

journal homepage: www.elsevier.com/locate/micres

Biodegradation of selected aminophosphonates by the bacterial isolate *Ochrobactrum* sp. BTU1

Ramona Riedel [a,*], Fabian M. Commichau [b,c,1], Dirk Benndorf [d,e,f,1], Robert Hertel [b,h], Katharina Holzer [g], Ludwig E. Hoelzle [g], Mohammad Saba Yousef Mardoukhi [a,b,c], Laura Emelie Noack [a], Marion Martienssen [a]

[a] Chair of Biotechnology of Water Treatment Brandenburg, Institute of Environmental Technology, BTU Cottbus-Senftenberg, Cottbus, Germany
[b] FG Synthetic Microbiology, Institute for Biotechnology, BTU Cottbus-Senftenberg, Senftenberg, Germany
[c] FG Molecular Microbiology, Institute for Biology, University of Hohenheim, Stuttgart, Germany
[d] Applied Biosciences and Process Engineering, Anhalt University of Applied Sciences, Köthen, Germany
[e] Chair of Bioprocess Engineering, Otto von Guericke University, Magdeburg, Germany
[f] Bioprocess Engineering, Max Planck Institute for Dynamics of Complex Technical Systems, Magdeburg, Germany
[g] Department of Livestock Infectiology and Environmental Hygiene, Institute of Animal Science, University of Hohenheim, Stuttgart, Germany
[h] Department of Genomic and Applied Microbiology, Institute of Microbiology and Genetics, Georg-August-University of Göttingen, Göttingen, Germany

ARTICLE INFO

Keywords:
Phosphonate
Biodegradation
EDTMP
Ochrobactrum
C-P Lyase
Sarcosine

ABSTRACT

Aminophosphonates, like glyphosate (GS) or metal chelators such as ethylenediaminetetra(methylenephosphonic acid) (EDTMP), are released on a large scale worldwide. Here, we have characterized a bacterial strain capable of degrading synthetic aminophosphonates. The strain was isolated from LC/MS standard solution. Genome sequencing indicated that the strain belongs to the genus *Ochrobactrum*. Whole-genome classification using pyANI software to compute a pairwise ANI and other metrics between *Brucella* assemblies and *Ochrobactrum* contigs revealed that the bacterial strain is designated as *Ochrobactrum* sp. BTU1. Degradation batch tests with *Ochrobactrum* sp. BTU1 and the selected aminophosphonates GS, EDTMP, aminomethylphosphonic acid (AMPA), iminodi(methylene-phosphonic) (IDMP) and ethylaminobis(methylenephosphonic) acid (EABMP) showed that the strain can use all phosphonates as sole phosphorus source during phosphorus starvation. The highest growth rate was achieved with AMPA, while EDTMP and GS were least supportive for growth. Proteome analysis revealed that GS degradation is promoted by C-P lyase via the sarcosine pathway, i.e., initial cleavage at the C-P bond. We also identified C-P lyase to be responsible for degradation of EDTMP, EABMP, IDMP and AMPA. However, the identification of the metabolite ethylenediaminetri(methylenephosphonic acid) via LC/MS analysis in the test medium during EDTMP degradation indicates a different initial cleavage step as compared to GS. For EDTMP, it is evident that the initial cleavage occurs at the C-N bond. The detection of different key enzymes at regulated levels, form the bacterial proteoms during EDTMP exposure, further supports this finding.

This study illustrates that widely used and structurally more complex aminophosphonates can be degraded by *Ochrobactrum sp.* BTU1 via the well-known degradation pathways but with different initial cleavage strategy compared to GS.

Abbreviations: AMPA, aminomethylphosphonic acid; AST, antibiotic susceptibility tests; AMR, antimicrobial resistance; DTPMP, diethylenetriamine penta (methylenephosphonic acid); t_d, doubling times; EABMP, ethylaminobis(methylenephosphonic) acid; EDTA, ethylenediaminetetraacetic acid; EDTMP, ethylenediaminetetra(methylenephosphonic acid); EPSP, 5-enolpyruvyl-shikimate-3-phosphate synthase; GS, glyphosate; μ_{max}, growth rate; IDMP, iminodi(methylenephosphonic); P_i, inorganic ortho-phosphate; PhnCDEFGHIJKLMNOP, multienzyme complex termed C-P lyase; *m/z*, mass to charge ratio; PhnA, phosphonoacetate hydrolase; PalH, phosphonopyruvate hydrolase; PhnX, phosphonoacetaldehyde hydrolase.

* Corresponding author.
E-mail address: ramona.riedel@b-tu.de (R. Riedel).
[1] Equal to first author

https://doi.org/10.1016/j.micres.2024.127600
Received 4 September 2023; Received in revised form 19 December 2023; Accepted 2 January 2024
Available online 8 January 2024

1. Introduction

The synthetic aminophosphonate ethylenediaminetetra(methylenephosphonic acid) (EDTMP) is characterized by four direct covalent carbon-to-phosphorus (C-P) bonds and two amino groups increasing its chemical stability (Obojska et al., 1999). EDTMP is applied as a transition metal chelator to protect bleaching agents from decomposing (Jaworska et al., 2002).

As recently reported, EDTMP is the structure-analogue of the already known ethylenediaminetetraacetic acid (EDTA). The difference between the two is that EDTMP forms multinuclear complexes thus, making the phosphonate extremely efficient. According to Studnik et al. (2015), a single EDTMP molecule can retain up to 5000–10 000 calcium ions in solution and prevent its precipitation. In comparison, EDTA forms stoichiometric complexes and considerable higher amount of EDTA are required yielding similar complexing properties and efficiencies.

Thus, EDTMP is a common component of detergent in households, which usually ends up in municipal wastewater. The removal of phosphonates such as EDTMP during wastewater treatment can vary greatly and different removal efficiencies depending on different phosphonates have been reported (Armbruster et al., 2020; Rott et al., 2018). For instance, a removal efficiency of up to 70% was recorded for EDTMP due to its adsorption onto activated sludge (Nowack, 1998). Thus, EDTMP removal during wastewater treatment is incomplete and the compound is continuously released to the aquatic environment. Like other chelating agents such as ethylenediaminetetraacetic acid (EDTA), it is expected that phosphonates will cause anthropogenic enrichment in streams over long time (Knepper, 2003). Since EDTMP has a long environmental lifetime, its negative impacts on the aquatic ecosystems are anticipated (Nowack, 2003; Lesueur et al., 2005; Rott et al., 2018).

The fate of EDTMP in the environment is still poorly understood. The reason for this could be the hard detection of highly polar aminophosphonates in aquatic solutions. Recently, different analytical methods based on liquid chromatography coupled mass spectrometry (LC/MS) analyses were reported for this specific compound group (Armbruster et al., 2020; Wang et al., 2019; Kuhn et al., 2017; Schmidt et al., 2014). Armbruster et al. (2020) were able to confirm the occurrence of EDTMP in natural water bodies and sediments. Unfortunately, the authors could not deliver further information on the potential biological degradation path of EDTMP. It is believed that photochemical degradation of phosphonates is the major pathway in aquatic environments while the occurrence of biodegradation occurs still underscored (Nowack, 2003; Kuhn et al., 2022). However, biodegradation of glyphosate (GS) in aquatic environment has often been reported (Grandcoin et al., 2017; Huntscha et al., 2018; Chen et al., 2022). Thus, biodegradation of other more complex synthetic aminophosphonates such as EDTMP is reasonable.

In recent years, a great number of studies have been investigating the enzymatic mechanism of how the C-P bond of phosphonates is cleaved (i.e., mainly without an amino group). Most of these studies were based on in vitro investigations and bacterial growth test (Pallitsch and Zechel, 2023; Ruffolo et al., 2023; Li et al., 2023; Ermakova et al., 2017; Kamat and Rauschel, 2013; McSorley et al., 2012; Sviridov et al., 2012; Villarreal-Chiu et al., 2012; Ternan et al., 1998). In many cases, it was reported that inducting phosphonate cleaving enzymes depends mainly on extracellular inorganic ortho-phosphate (P_i) uptake and/or P_i starvation. Hsieh and Wanner (2010) reviewed in detail the biochemical mechanism of the phosphate (Pho) starvation regulon including signal transduction under conditions of surplus P_i and P_i limitation. Villarreal-Chiu et al. (2012) pointed out that the enzymatic regulation of the C-P cleavage during available P_i uptake and/or P_i starvation are both under direct control of the Pho regulon, which is controlled by the PhoR/PhoB two-component system in many biological systems. According to Hsieh and Wanner (2010) almost all genes directly controlled by the PhoR/PhoB are associated with P_i assimilation or alternative P sources for bacterial growth. Therefore, biodegradation of synthetic phosphonates is presumed to require a specific condition inducing the Pho regulon.

At least three different enzymatic cleavage mechanisms for phosphonates were recently reported including: (i) the hydrolytic cleavage catalyzed by the enzymes phosphonoacetate hydrolase (PhnA), phosphonopyruvate hydrolase (PalH) and phosphonoacetaldehyde hydrolase (PhnX); (ii) the oxidative cleavage mediated by enzymes termed phosphonatase (PhnY and PhnZ); and (iii) the radical-mediated cleavage carried out by the multienzyme complex termed C-P lyase (PhnCDEFGHIJKLMNOP) (Horsman and Zechel, 2017). Both the hydrolytic and oxidative pathway show commonly a narrow substrate specific spectrum mainly prevalent for organophosphonates (Horsman and Zechel, 2017; McSorley et al., 2012). In contrast, the C-P lyase mediated pathway shows a broad and more unspecific substrate spectrum including both organo- and aminophosphonates. The C-P lyase catalyzes a radical-based homolytic cleavage of the C-P bond (Metcalf and Wanner, 1993). This enzyme complex has been studied deeply for more than three decades (Zhang and Van der Donk, 2013; Metcalf and Wanner, 1993). A very detailed description of the entire pathway with every single reaction stage is shown by Kamat and Raushel (2013). Meanwhile, different types of the C-P lyase have been identified and described (Sviridov et al., 2012).

Regarding biodegradation of synthetic aminophosphonates such as EDTMP, the C-P lyase seems to be predestined and having the potential to break down those long-lasting structures. However, up to date, biodegradation of EDTMP based on microbial C-P lyase has not been reported. We, recently, isolated a bacterial strain indicating biodegradation of synthetic aminophosphonate diethylenetriamine penta(methylenephosphonic acid) (DTPMP) and EDTMP but without evidence of the enzymatic pathway mediated during biodegradation (Riedel et al., 2023). Thus, the aim of the study was to investigate more in detail the potential of *Ochrobactrum* sp. BTU1 toward biodegradation of selected aminophosphonates. We carried out specific biodegradation tests allowing to determine not only the specific growth rate (μ_{max}) and doubling times (t_d), but also, to perform LC/MS analyses detecting the reduction of mother compounds in cell-free media. We determined the degradation curves of EDTMP as well as of aminomethylphosphonic acid (AMPA), iminodi(methylene-phosphonic) acid (IDMP), and ethylaminobis(methylenephosphonic) acid (EABMP). The latter, i.e., AMPA, IDMP and EABMP, are common breakdown products of photochemical treatments. For better comparison, we also performed degradation tests with GS. Strain characterization was performed by initial taxonomic classification and whole-genome sequencing, in silico antimicrobial resistance (AMR) and virulence determination, antibiotic susceptibility tests (AST) and proteomic analyses identifying key enzymes related to the potential catabolic pathway.

2. Material and methods

2.1. Chemicals, reagents, and bacterial culture media

EDTMP and EABMP were provided by "Zschimmer & Schwarz Mohsdorf" (Burgstädt, Germany). IDMP and AMPA were purchased from Sigma Aldrich (Steinheim, Germany). The chemical structure of all phosphonates is presented below (Fig. 1). Ultra-pure water (LC/MS grade) was in-house generated (Adrona Sia Crystal EX, Lithuania). Acetonitrile of LC/MS grade was purchased from VWR (Dresden, Germany), ammonium acetate and ammonium formate of analytical grade were purchased from VWR (Leuven, Belgium). All other solvents and chemicals were purchased from Fluka/Riedel-de Haën/Sigma-Aldrich (Taufkirchen, Germany), or from Merck VWR (Darmstadt, Germany), respectively. The cation exchange resin Dowex 50WX8 with 100–200 mesh (hydrogen form) was purchased from Acros Organics (Geel, Belgium). All chemicals used were of analytical grade or better with purity > 99%. Bacteria were grown in lysogeny broth (LB) and Nutrient broth II (NB II, Sifin, Germany). Agar (Roth Germany) was added when required.

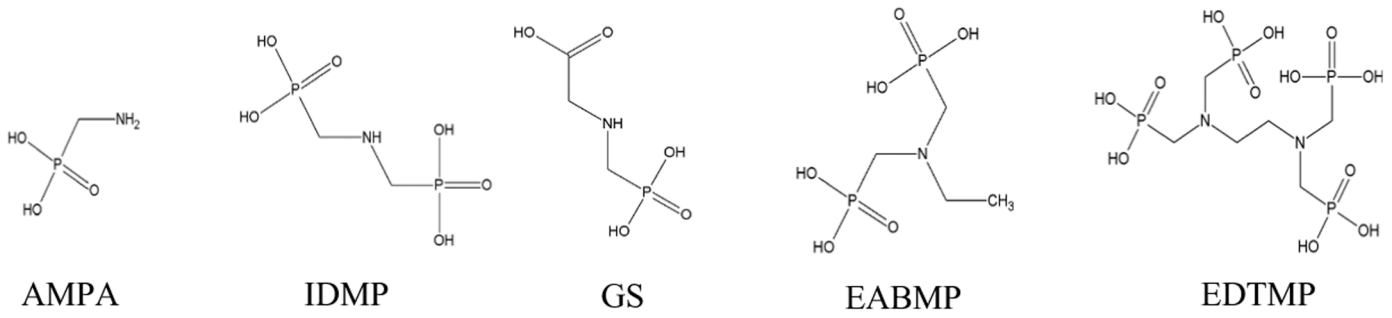

Fig. 1. Chemical structures of the aminophosphonates used in the degradation assays. Aminomethylphosphonic acid (AMPA), iminodi(methylene-phosphonic) (IDMP), glyphosate (GS), ethylaminobis(methylene-phosphonic) acid (EABMP) and ethylenediaminetetra(methylenephosphonic acid) (EDTMP).

2.2. Isolation of the phosphonate-degrading bacterial strain

A diethylenetriamine penta(methylenephosphonic acid) (DTPMP) LC/MS standard contaminated with bacteria was used for bacterial isolation of strain *Ochrobactrum* sp. BTU1. Spot of well suspended DTPMP standard solution were placed on nutrient agar and incubated at room temperature for three days. Single colonies were further picked and strike out on fresh nutrient agar plates. Sequential passages on DTPMP standard solution supplemented with ammonium acetate as nitrogen and carbon source were performed until pure cultures were isolated by spotting on nutrient agar plates incubated at room temperature. Potential biodegradation of synthetic aminophosphonates was then proven by performing biodegradation tests.

2.3. Taxonomic classification of the bacterial isolate

Total nucleic acids were extracted using the MasterPureTM DNA purification kit (Epicentre, Madison, WI, USA) and used for the initial taxonomic classification and genome sequencing (see below). Initial taxonomic classification of the bacterium isolated from the DTPMP LC/MS standard was realized by sequencing the 16 S rRNA gene, which was amplified by PCR using the primers 27 F (5'-AGAGTTTGATCMTGGCTCAG) and 1429 R (5'-TACGGYTACCTTGTTACGACTT) (Frederikson et al., 2013). The tool pyANI v. 0.2.10 (https://github.com/widdowquinn/pyani#conda, accessed on 19 June 2021) is a module for whole-genome classification of microbes using average nucleotide identity. This module was used to compute a pairwise ANI and other metrics between *Brucella* assemblies and *Ochrobactrum* contigs.

2.4. Whole-genome sequencing and bioinformatic procedure of the raw reads

Genomic library preparation and total genomic DNA sequencing were performed by Azenta (Leipzig, Germany). The libraries were sequenced using Illumina Novaseq 6000, theoretically producing at least 5 million 151 bp paired-end reads. High-throughput short-read sequencing yielded 19770858 reads for *Ochrobactrum* sp. BTU1 leading to a coverage of 823 (Genome characteristics are listed in Table S1). For analyzing the WGS data in a standardized and automated manner, the Linux-based bioinformatic WGSBAC (v.2.1) pipeline (https://gitlab.com/FLI_Bioinfo/WGSBAC/-/tree/version2, accessed on 15 June 2022) was used. The pipeline input consisted of a metadata file and the Illumina paired-end fastq files. Raw coverage for each dataset was calculated by the number of reads multiplied by their average read length and divided by the genome size. Contigs were assembled using Shovill v.1.0.4 (https://github.com/tseemann/shovill, accessed on 15 June 2022), an optimizer for SPAdes assembler (Bankevich et al., 2012). Quality control of the assembled contigs was performed by QUAST v. 5.0.2 (Gurevich et al., 2013).

Identifying the potential virulence-associated determinants was retrieved from the virulence factor database (VFDB, http://www.mgc.ac.cn/VFs/, accessed on 19 June 2022) using the core dataset (Liu et al., 2019). All fastq files were submitted to the National Center for Biotechnology Information (NCBI) under the BioProject number PRJNA733446 (https://www.ncbi.nlm.nih.gov/bioproject/?term=BTU1).

2.5. Exclusion of Brucella pathogens

To exclude our isolate BTU1 might be a *Brucella* isolate, primers B4 (5'-TGGCTCGGTTGCCAATATCAA) and B5 (5'-CGCGCTTGCCTTTCA GGTCTG) for the *Brucella* specific gene bcsp31 were tried to hybridize in silico using Geneious v.11.1.5 (https://www.geneious.com/, accessed on 15 June 2022) with the DNA sequence of the assembled contigs as calculated by Shovill in the bioinformatic pipeline.

2.6. In silico AMR and virulence determination

In silico detection of AMR genes was performed using the Resistance Gene Identifier (RGI) based on the Comprehensive Antibiotic Resistance Database (CARD) (Jia et al., 2017). Identifying the potential virulence-associated determinants was retrieved from the virulence factor database (VFDB, http://www.mgc.ac.cn/VFs/) using the core dataset (Liu et al., 2019).

2.7. Antibiotic susceptibility tests

ASTs were performed *via* a disc diffusion assay (Hertel et al., 2022). Briefly, the bacteria to be tested were cultured overnight in 4 mL LB medium at 28 °C at 220 rpm. On the next day, the bacteria were washed twice in 0.9% (w/v) NaCl solution and 100 µL of the cell suspensions were propagated on LB agar plates. Cotton disks (Roth, Germany) containing 5 µL of the antibiotic solutions (penicillin G (100 mg mL^{-1}), ampicillin (100 mg mL^{-1}), polymyxin (10 mg mL^{-1}), ciprofloxacin (1 mg mL^{-1}), doxycyclin (6 mg mL^{-1}), gentamycin (2 mg mL^{-1}), kanamycin (50 mg mL^{-1}), spectinomycin (100 mg mL^{-1}), streptomycin (100 mg mL^{-1}), tetracyclin (20 mg mL^{-1}), chloramphenicol (5 mg mL^{-1}), lincomycin (25 mg mL^{-1}), erythromycin (2 mg mL^{-1}), sulfonamide (60 mg mL^{-1})) were placed in the center of the plates which were incubated for 24 h at 37 °C. For evaluating the antibiotic susceptibilities, the zone of inhibition was measured.

2.8. Phosphonate degradation test sample and preparation for proteomic analyses

A single colony was used to inoculate 5 mL NB II medium under strict phosphorus limiting conditions, for the biodegradation test. The preculture 1 was incubated overnight at 180 rpm and room temperature (RT). Next, 250 µL of preculture 1 with an optical density at 660 nm (OD_{660}) > 0.6 were used to inoculate 250 mL NB II medium. The preculture 2 was incubated overnight at 180 rpm and RT. Next, bacteria were harvested by centrifugation (10 min, 5.000 x g, RT). For the biodegradation test, the cell pellet was washed three times with 0.9%

NaCl. Bacteria were resuspended in 20 mL freshly prepared defined medium containing 55.6 mg L^{-1} $CaCl_2$, 234.5 mg L^{-1} $MgSO_4$ x 7 H_2O, 4000 mg L^{-1} NH_4COOCH_3, 12.5 mg L^{-1} $KHCO_3$ and 1 mL trace metal solution (SL-8) with EDTA (Pfennig and Trüper, 1981). After adjusting the pH to 7.2, the medium was sterilely filtrated using a sterilized cellulose nitrate filter with a pore size of 0.2 µm (Sartorius, Göttingen, Germany). The washed bacteria were used to inoculate three flasks containing 250 mL medium to an OD_{660} of 0.1. The OD was measured using a Beckmann DU 600 spectrophotometer (Fullerton, USA). To achieve phosphorous limitation of the cells, the three flasks (precultures 3) were incubated for one week at 180 rpm and RT. After starvation, each culture reached an OD_{660} of around 0.5. For the biodegradation test, seventeen sterile flasks were prepared by diluting pre-culture 3 with fresh degradation media to an OD_{660} of 0.1. Each aminophosphonate was prepared in triplicates, i.e., a total of fifteen flasks were supplemented either with 100 mg L^{-1} GS (18 mgP L^{-1}), 100 mg L^{-1} EDTMP (28 mgP L^{-1}), 100 mg L^{-1} AMPA (28 mgP L^{-1}), 100 mg L^{-1} IDMP (30 mgP L^{-1}), or 100 mg L^{-1} EABMP (27 mgP L^{-1}). The positive control containing fresh diluted bacteria was supplemented with 100 mg L^{-1} KH_2PO_4 (22.8 mgP L^{-1}) as sole phosphorus source. The negative control containing fresh diluted bacteria was inoculated without additional phosphorus sources. Bacterial growth was monitored by measuring the OD_{660} and μ_{max} and t_d. Biodegradation was monitored by collecting once a day 6 mL sample of each flask. These samples were centrifuged (10 min, 17, 000 x g, 4 °C). The supernatants were collected and stored in plastic tubes at 4 °C prior to additional sample clean-up, followed by LC/MS analyses.

For proteomic analyses, bacterial samples were taken from preculture 3 that was incubated for one week and from the biodegradation cultures at an OD_{660} of 0.5 for all investigated aminophosphonates and the positive control. All samples were taken in triplicates.

Purity control was always carried out at the beginning and at the end of each biodegradation test by spotting 10 µL bacterial suspension on nutrient agar plates and incubating at room temperature for at least two days.

2.9. Analysis of EDTMP and its degradation products by LC/MS

EDTMP and its degradation products were analyzed with liquid chromatography-electro spray ionization-mass spectrometry (LC-ESI-MS) using a Finnigan MAT LC/MS (LC spectral system P4000, LCQ MS Detector, autosampler AS 3000, PEEK column SeQuant ZIC-HILIC 150 × 2.1 mm, 3.5 µm/100 Å, Merck, Darmstadt, Germany). Prior to the analyses, all collected samples were purified by applying our optimized clean-up procedure with cation exchange resin Dowex 50WX8 having an exchange wet volume capacity of 1.7 meq mL^{-1} (Kuhn et al., 2020). Subsequently, all liquid samples were mixed with 50% acetonitrile. The gradient elution was performed with solvent A (100% ultra-pure water) and solvent B (10% ultra-pure water/90% acetonitrile) at 35 °C at a flow rate of 0.2 mL min^{-1}. Solvents A and B contained 100 mM and 2.5 mM ammonium formate, respectively. The analysis was ran for 43 min by first holding 100% of solvent B for 2 min. The gradient was then concavely increased to 10% A for 1 min and was held for 2 min. The gradient was further concavely increased to 30% A for 1 min and held again for 2 min. Subsequently, the gradient was again concavely increased to 50% A for 2 min and held for 10 min. Afterwards, the gradient was concavely increased to 60% A for 5 min and held for another 5 min, before the gradient was concavely increased back to 100% B for 3 min and held for 10 min. The MS detector settings were as follows: The negative polarity ionization was 3.5 kV and the spray capillary temperature was 220 °C. Selected-ion monitoring (SIM) was selected for quantification. The following mass-to-charge (m/z) ratios were used for identification: EDTMP 435, EABMP 232, IDMP 204, GS 168 and AMPA 110. For qualitative analyses, full MS scan was used with a mass range between m/z 90 to 650.

2.10. Identification and quantification of proteins by LC-MS/MS based proteomics

During the exponential growth phase, biomass from degradation experiments were collected by centrifugation (17000 x g, 10 min, 4 °C) of the complete degradation medium. Cells were inactivated and lysed by incubation of 1 mL cell pellet in 5 mL SDS lysis buffer (2% SDS in 20 mM Tris/HCl pH 7.5) for 2 min at 95 °C. Lysed cell were transferred to mass spectrometry lab. Lysates were homogenized in a bead mill (FastPrep 96, MP Biomedicals) at 1800 min^{-1} for 20 min. After centrifugation (1 min, 8500 x g, 4 °C) 150 µL supernatant were mixed with 1.5 mL DNase (0.1 mg mL^{-1} $MgCl_2$ +1 mM PMSF + 1 µL mL^1 Cyanase (Unicersal Biologics) in 20 mM Tris/HCl pH 7.5). The suspension was incubated for 10 min (37 °C, 1400 min^{-1}) and then centrifuged for 10 min (8500 x g, 4 °C). The supernatants were stored at − 18 °C for subsequent use. Protein concentration was determined with amido black and bovine serum albumin as standard protein (Heyer et al., 2019). 100 µg proteins were submitted to filter assisted sample preparation (Wiśniewski et al., 2009) as previously described (Heyer et al., 2019). Protein identification was carried out using an UltiMate® 3000 nano splitless reversed phase nanoHPLC (Thermo Fisher Scientific) coupled to timsTOF Pro mass spectrometer (Bruker Daltonik GmbH) (Küchler et al., 2023). Data from measurement in PASEF and SWATH mode were processed with MASCOT and Skyline (Küchler et al., 2023) using the sequenced genome as database for protein identification. The parameters in Skyline were set to "enzyme = trypsin", "maximal missed cleavages = 1", and "structural modifications = carbamidomethyl (cysteine), oxidation (methionine)". The peptide areas were exported as CSV files. Validated peptides (q-value 0.05) were processed for further analysis in Microsoft Excel.

The volume of peptides was normalized to the total volume of each sample after the background had been corrected. Samples in triplicates were used to calculate the induction ratios (log_2). Samples that had phosphates were used as positive control for the growth tests. The t-test (p-value < 0.05) was used to filter significant changes in the samples.

3. Results

3.1. Isolation of a bacterial strain from a phosphonate standard solution

We isolated bacterial strain *Ochrobactrum* sp. BTU1 from our LC/MS standard solution containing DTPMP. The standard solution had a stock concentration of 100 mg L^{-1} DTPMP solubilized in ultra-pure water. The unbuffered DTPMP solution had a pH value of 3.5 and was stored continuously in the dark at 4 °C in a sealed glass vessel. After six weeks of undisrupted storage, slight microbial contaminations were visible when shaking the glass vessel. From the contaminated DTPMP stock solution, bacterial colonies with different morphologies were isolated after incubated on agar plates. One bacterial isolate dominated the microbial population on the plates. Therefore, we decided to characterize and investigate the potential of this strain to biodegrade selected aminophosphonates.

To assess the growth characteristics of *Ochrobactrum* sp. BTU1, the strain was grown in NB II liquid medium at RT and at 37 °C (Fig. S1). The strain grew slightly faster at 37 °C. At RT, we determined a bacterial growth rate μ_{max} of 9.1 ± 0.1 $days^{-1}$ corresponding to a doubling time of 109.2 ± 0.9 min. For 37 °C, we determined a bacterial growth rate μ_{max} of 11.1 ± 0.1 $days^{-1}$ corresponding to a doubling of 89.9 ± 0.5 min

3.2. 16 S rRNA and genome sequencing analysis and strain characterization

To avoid working with a potentially harmful bacterial isolate, we performed an initial taxonomic classification by determining the 16 S rRNA sequence. The sequencing analysis revealed that the bacterial isolate belongs to the genera *Brucella* or *Ochrobactrum* (Table S2). Both

Table 1
Features of the draft genome of *Ochrobactrum* sp. BTU1.

Chromosome	Accession number	Size [bp]	GC content [%]
1	NZ_CP076354.1	2371,342	53.6
2	NZ_CP076355.1	1663,974	52.6
3	NZ_CP076356.1	1003,303	51.5
4	NZ_CP076357.1	840,417	51.0

bacteria belong to the α-proteobacteria family (Dorsch et al., 1989; Moreno et al., 1990; Velasco et l., 1998) and are closely related but differ in their genome size (*Brucella*: 3.1–3.4 Mb vs. *Ochrobactrum*: 4.7–8.3 Mb) (Moreno et al., 2022). While the *Brucella* group is responsible for the zoonosis brucellosis and comprises intracellular pathogens, *Ochrobactrum* is a diverse group of free-living bacteria with a few species occasionally infecting immunocompromised patients (Moreno et al., 2022). Recently, certain *Ochrobactrum* species were incorrectly included in the genus of *Brucella* based on a BLAST Distance Phylogeny approach (Hördt et al., 2020). This is the reason, why some *Ochrobactrum* species are listed as *Brucella* in NCBI erroneously. However, it has been suggested that *Brucella* and *Ochrobactrum* organisms must be maintained apart in two different genera (Moreno et al., 2022; Holzer et al., 2023). To get further insights into the identity of our bacterial isolate, we performed Illumina sequencing and assembled a draft genome (Table 1). The genome was predicted to contain 5485 genes, among them 5292 protein coding genes and 110 pseudo genes. An additional alignment by pyANI with all available *Brucella* species sequences that were downloadable from GenBank and *Ochrobactrum* with BTU1 clearly demonstrated the conserved *Brucella* genome within all *Brucella* species, showing a nucleotide identity of 99.8 - 97.8% (Table S3). In comparison, our strain BTU1 showed a nucleotide identity of 82.9–83.8% to these *Brucella* species. Therefore, it can be ruled out that BTU1 belongs to the *Brucella* genus. Thus, from now on, our bacterial isolate is designated as *Ochrobactrum* sp. BTU1. This is further confirmed by the genome size of 5.7 Mb, the absence of the *Brucella* specific bscp31 gene, as mentioned before, and the absence of important virulence and surviving factors of *Brucella* like their VirB system (Delrue et al., 2001). To be more specific, the *Brucella* VirB T4SS serves as a critical factor for virulence, playing vital roles in facilitating intracellular survival and manipulating the host's immune response during infection. Brucella induces host pathogenesis by thriving and replicating within specific target cells, a process that relies on the VirB operon-encoded T4SS (Njeru et al., 2016). This VirB system in *Brucella* spp. demonstrates a high conservation (Ke et al., 2015). The expression of the VirB system is regulated by environmental signals (Boschiroli et al., 2002). In BTU1, however, no genes related to VirB1-VirB12 were found in the isolate. Further, genes that are not contained in the genome of BTU1 but that are specific for *Brucella*, are a number of genes important for a special lipopolysaccaride establishment (Lapaque et al., 2005). These occur in *Brucella* and the multiple peptide resistance factor (*mprF*) encoding an integral protein, which modifies anionic phosphatidylglycerol for repulsion of cationic antimicrobial peptides (CAMPs) leading to a resistance to CAMPs (Ernst et al., 2009) (Table S4).

Next, we examined whether the bacteria are resistant to antimicrobial substances by performing ASTs. For this purpose, we determined the zone of inhibitions around filter discs containing antibiotics targeting the cell envelope, DNA condensation/segregation, translation, and cofactor synthesis. As shown in Fig. 2, *Ochrobactrum* sp. BTU1 was only resistant to sulfonamide that inhibits biosynthesis of folic acid (Achari et al., 1997). In comparison to *Burkholderia* (β-proteobacteria), *Escherichia coli* (γ-proteobacteria) and *Bacillus subtilis* (*bacilli*) strains (Hertel et al., 2022), *Ochrobactrum* sp. isolate BTU1 (α-proteobacteria) shows an increased antibiotic susceptibility.

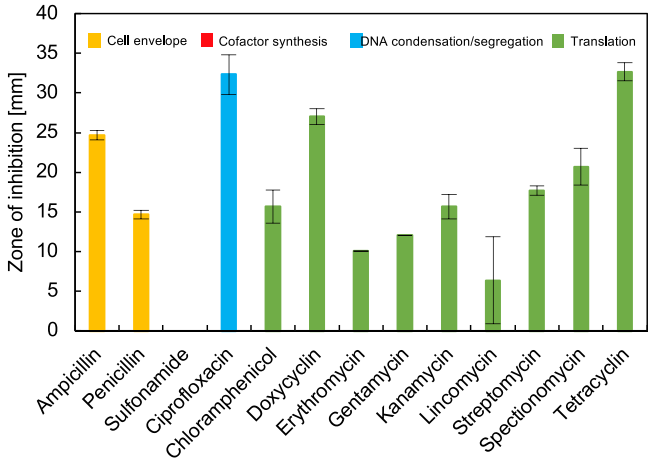

Fig. 2. Antibiotic susceptibility tests. Error bars represent standard errors of means of triplicate plating experiments.

3.3. Degradation of selected aminophosphonates

We performed biodegradation tests with the bacteria strain using the aminophosphonates GS, EDTMP, AMPA, IDMP, and EABMP as a sole P source but carbon. No additional P_i or alternative P sources were available. To prevent bacterial growth by utilizing intracellular stored P sources, we starved the bacteria seven days before addition of 100 mg L^{-1} of each aminophosphonates. During the starvation time, the OD_{660} of the bacterial suspension increased from 0.1 to approximately 0.3. Microscopic observation indicated that bacterial cells had intensively elongated but the cell number was not significantly increased (Fig. S1).

Our results of the biodegradation test demonstrate that our bacteria strain was capable to grow on all five aminophosphonates as a sole P source (Fig. 3). We determined different lag-phases for the five aminophosphonates. Thus, the longest lag-phase occurred for the largest aminophosphonates EDTMP followed by EABMP and IDMP. The shortest lag-phase occurred for AMPA and GS, like the positive control. Our results from LC/MS analyses confirm that the concentration all mother compounds during the biodegradation tests decreased within the individual test time. Interestingly, we found EDTMP drastically reduced within the first day and later again from day 6 to 8 when the bacteria strain grew exponentially (Fig. 3A). During the lag-phase and the initial exponential growth phase, EDTMP concentration was found to decrease only minimally. In comparison, we determined continuous and fastest decrease of AMPA (Fig. 3B). The decrease of EABMP and IDMP (Fig. 3C & D) was significantly slower compared to AMPA but more straight as compared with EDTMP. The decrease of GS was among the lowest of all five aminophosphonates tested (Fig. 3E).

Based on our determined growth curves, we calculated the specific growth rates and doubling times for each aminophosphonate and the positive control (Table 2). We found the slowest growth rate, μ_{max} and its corresponding longest doubling time, t_d for EDTMP and glyphosate. In contrast, we determined the fastest growth rate, μ_{max} and the shortest doubling time, t_d for AMPA. Our determined doubling time, t_d for the five aminophosphonates indicated a clear trend from shortest to longest t_d: AMPA<IDMP<EABMP<EDTMP<GS. Thus, AMPA showed the shortest t_d of all five tested aminophosphonates.

However, in comparison to our positive control, t_d of AMPA was almost doubled indicating inhibited growth. We calculated the ratio (P/S) between t_d of the positive control (P) and the investigated substrate (S), i.e., the individual aminophosphonates investigated. The P/S gave a better comparison of our data and final interpretation of determined growth rates (Table 2). The results of the P/S ratio clearly indicates that the lowest growth and biodegradation in terms of C-P cleavage occurred in EDTMP and glyphosate.

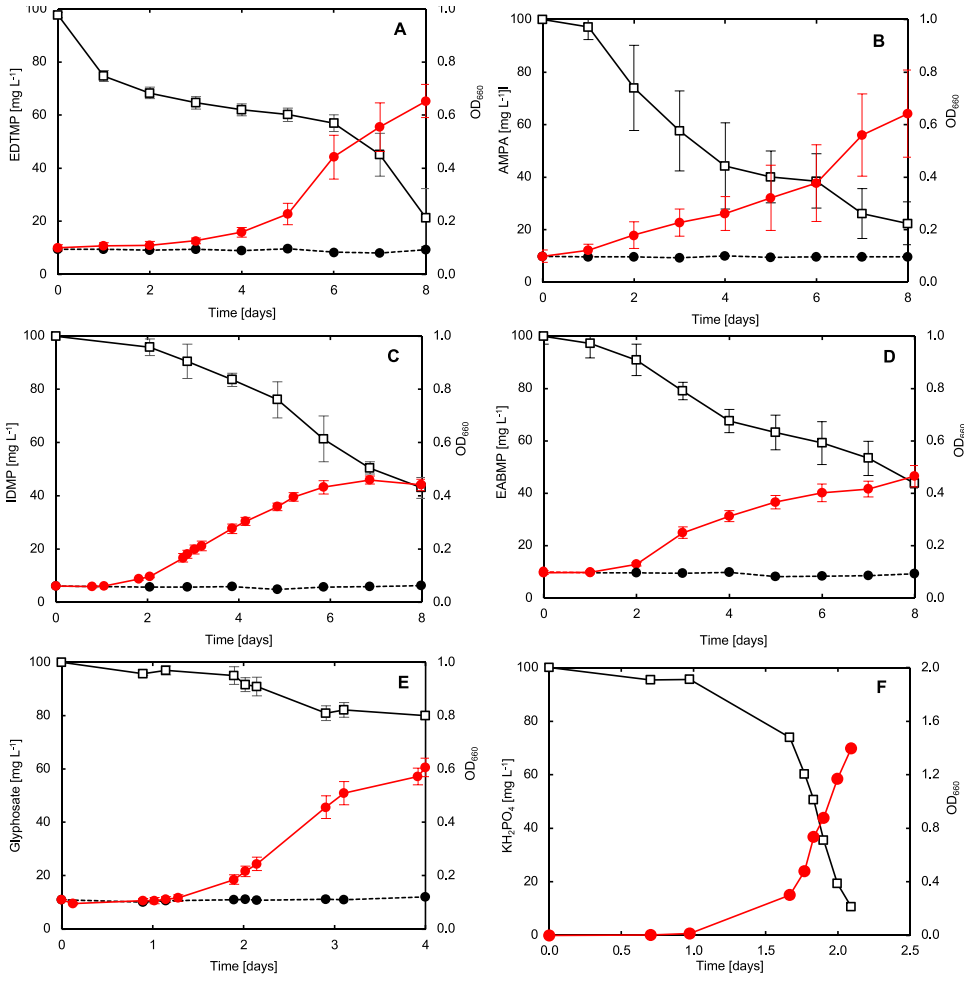

Fig. 3. Growth of *Ochrobactrum* sp. BTU1 with aminophosphonates as the source of phosphorous and ammonium acetate as nitrogen and carbon source, respectively. Black line with squares represents biodegradation curve of the selected aminophosphonate. Red line with circles represents bacterial growth curve. Dashed lines in square dot represent the biological negative control, i.e., no addition of phosphorus. (A) Biodegradation of EDTMP. (B) Biodegradation of AMPA. (C) Biodegradation of IDMP. (D) Biodegradation of EABMP. (E) Biodegradation of GS. (F) Positive control with addition of KH_2PO_4 as a sole phosphorus source.

Table 2
Growth rates of *Ochrobactrum* sp. BTU1 obtained during cultivation with selected aminophosphonates.

P sole source	μ_{max} [d^{-1}]	t_d [h]	P/S* [-]
GS	0.54 ± 0.09	30.7 ± 4.4	0.36 ± 0.1
EDTMP	0.56 ± 0.08	30.3 ± 4.0	0.37 ± 0.1
AMPA	0.80 ± 0.09	20.9 ± 2.1	0.57 ± 0.1
IDMP	0.72 ± 0.07	23.3 ± 2.4	0.58 ± 0.1
EABMP	0.65 ± 0.09	25.9 ± 3.8	0.56 ± 0.1
KH_2PO_4	1.55 ± 0.18	11.0 ± 1.4	-

* ratio between t_d of the positive control (P) and the investigated substrate (S).

We also analyzed our LC/MS samples for breakdown products like those occurring during photochemical degradation and others. For EDTMP, we neither detected formation of EABMP, IDMP nor AMPA in the cell free test medium. Also, for EABMP and IDMP, we did not detect standardized breakdown products such as IDMP and/or AMPA, respectively. Using LC/MS full scan, additional transformation products were further detectable as *m/z* ratios, but none of them was quantifiable due to the lack of standards. GS and AMPA were excluded from these analyses because the sample clean-up method was unfortunately not suitable. Therefore, we only analyzed the intensity developments via LC/MS from the samples of the biodegradation tests of EDTMP, IDMP and EABMP (Fig. S3-5). We detected for EDTMP three relevant *m/z* ratios, i.e., *m/z* 145, *m/z* 188 and *m/z* 341 (Fig. S3).

We previously identified *m/z* 341, being the phosphonate structure ethylenediaminetri(methylenephosphonic acid) (Kuhn et al., 2017). The formation and slight enrichment of ethylenediaminetri(methylenephosphonic acid) in the medium was continuous until day 6 and afterwards decreased rapidly. For IDMP, we detected the relevant *m/z* ratios 145, 191, 333 and 345 (Fig. S4). For EABMP, we also detected the relevant *m/z* ratios 145, 191 and 345 (Fig. S5). Their identification is still under progress. We also analyzed the presence of residual P_i in the cell free test medium. Our results clearly indicated that extracellular P_i was never detectable for none of the tested phosphonates.

3.4. Proteomic analyses of Ochrobactrum sp. BTU1 during cultivation with selected aminophosphonates

To identify the proteins and enzymes that are potentially involved in the degradation of the investigated aminophosphonates and possible release of phosphate, a proteomic analysis was carried out using cell pellets that were obtained from biodegradation tests. Based on the genome sequence, we could assign the identified proteins to the corresponding genes and genomic loci. Table 3 shows proteins whose amount changed during cultivation with all five phosphonates as well as proteins related to phosphate and phosphonate metabolism, with phosphate as a control for the calculation of induction rate. Specific effects of individual aminophosphonates are shown elsewhere (Table S5).

Table 3
Changes in the proteome of *Ochrobactrum* sp. BTU1 during growth with selected aminophosphonates. The volume of peptides was normalized to the total volume of each sample after the background had been corrected. Samples in triplicates were used to calculate the induction ratios (log_2). Samples that had phosphates were used as positive control for the growth tests. Significant changes were filtered by t-test (p-value < 0.05). '-' marks non-significant ratios.

				Log_2 [aminophosphonate/positive control]				
Protein	**Locus tag**	**Functional category**	**Function**	**AMPA**	**GS**	**IDMP**	**EABMP**	**EDTMP**
DNA polymerase subunit	KMS41_00100	Information Profession	DNA polymerase γ/τ subunit, DNA polymerization	-2.43	-1.89	-3.39	-1.53	-2.71
CysQ	KMS41_00945	Metabolism	3'(2'),5'-bisphosphate nucleotidase, sulfate assimilation	-1.50	-1.15	-2.02	-2.69	-1.53
Sarcosine oxidase subunit	KMS41_01085	Metabolism	Sarcosine oxidase β subunit, sarcosine degradation	-1.56	2,59	-3.03	-	-3.12
Sarcosine oxidase subunit	KMS41_01090	Metabolism	Sarcosine oxidase δ subunit, sarcosine degradation	-	2.60	-	-	1.74
Sarcosine oxidase subunit	KMS41_01095	Metabolism	Sarcosine oxidase α subunit, sarcosine degradation	4.39	4.50	3.02	4.96	-
Sarcosine oxidase subunit	KMS41_01100	Metabolism	Sarcosine oxidase γ subunit, sarcosine degradation	1.50	2.99	1.65	-	2.42
Pgi	KMS41_01400	Metabolism	Glycolysis	2.41	1.22	3.16	2.85	2.60
Uncharacterized	KMS41_01590	Unknown	Unknown	1.98	3.00	2.43	2.95	1.68
Ppk	KMS41_03530	Metabolism	Polyphosphate kinase, polyphosphate synthesis	4.30	2.76	4.98	4.23	4.78
RibE	KMS41_03620	Transport	6,7-Dimethyl-8-ribityllumazine synthase, riboflavin biosynthesis	4.30	2.76	4.98	4.23	4.78
duf_{1045}	KMS41_04135	Metabolism	DUF1045 domain-containing protein	1.30	-	1.92	2.13	2.07
PhnM'	KMS41_04140	Metabolism	Alpha-D-ribose 1-methylphosphonate 5-triphosphate diphosphatase, phosphonate degradation					
PhnE	KMS41_05445	Transport	ABC transporter permease subunit, phosphonate transport	-	-	-	-	-
PhnE'	KMS41_05450	Transport	ABC transporter permease subunit, phosphonate transport	-	-	-	-	-
PhnD	KMS41_05455	Transport	ABC transporter periplasmic binding protein, phosphonate transport	5.29	4.39	4.59	6.91	5.04
PhnC	KMS41_05460	Transport	ABC transporter nucleotide binding protein, phosphonate transport	3.63	2.39	4.29	6.21	4.20
PhnN	KMS41_05465	Metabolism	Ribosyl bisphosphate phosphokinase, phosphonate degradation	-	3.39	-	-	-
PhnM	KMS41_05470	Metabolism	5-Triphosphoribosyl 1-phosphonate diphosphohydrolase, phosphonate degradation	5.08	5.95	6.04	5.69	4.59
PhnO	KMS41_05475	Metabolism	Aminoalkylphosphonate *N*-acetyl-transferase, phosphonate degradation	7.58	8.56	8.58	7.92	8.12
PhnL	KMS41_05480	Metabolism	Phosphonate C-P lyase system protein, phosphonate degradation	7.07	8.77	8.34	7.85	7.54
PhnK	KMS41_05485	Metabolism	Phosphonate C-P lyase system protein, phosphonate degradation	6.52	7.77	8.41	7.57	7.31
PhnJ	KMS41_05490	Metabolism	Phosphonate C-P lyase, phosphonate degradation	7.53	8.64	9.14	8.39	7.89
PhnI	KMS41_05495	Metabolism	Phosphonate C-P lyase system protein, phosphonate degradation	6.96	8.94	9.11	7.94	8.36
PhnH	KMS41_05500	Metabolism	Phosphonate C-P lyase system protein, phosphonate degradation	4.70	7.13	6.68	-	7.11
PhnG	KMS41_05505	Metabolism	Phosphonate C-P lyase system protein, phosphonate degradation	9.02	9.73	10.30	9.39	9.82
PhnF	KMS41_05510	Transcription regulation	Transcriptional regulator of phosphonate degradation genes	-	-	-	-	-
Uncharacterized	KMS41_06595	Metabolism	3-Hydroxyisobutyrate dehydrogenase, amino acid catabolism?	-2.13	-1.49	-2.37	-2.02	-3.44
Uncharacterized	KMS41_06735	Transport	ABC transporter periplasmic binding protein, sugar transport?	2.26	1.64	2.56	3.32	2.45
Uncharacterized	KMS41_07420	Metabolism	Putative metallophosphoesterase, unknown function	4.77	4.38	4.44	6.44	4.25
Uncharacterized	KMS41_07440	Transport	ABC transporter periplasmic binding protein, sugar transport?	5.98	5.33	6.87	7.31	6.34
FliJ	KMS41_07930	Motility	Flagellar export protein	-1.55	-2.41	-2.00	-2.87	-1.12
Uncharacterized	KMS41_08025	Transport	ABC transporter periplasmic binding protein, sugar transport?	3.12	2.85	3.89	4.55	3.87
Ppa	KMS41_08985	Metabolism	Inorganic pyrophosphatase, catalyzes hydrolysis of pyrophosphate	10.03	8.90	10.48	10.72	10.30
Uncharacterized	KMS41_10935	Transport	ABC transporter periplasmic binding protein	6.65	6.63	7.63	8.92	7.00
UgpQ	KMS41_10960	Metabolism	Glycerophosphodiester phosphodiesterase, carbon metabolism	6.11	6.95	6.72	8.17	6.12
Uncharacterized	KMS41_10965	Metabolism	Sugar phosphate isomerase/epimerase, carbon metabolism	4.56	3.26	6.01	6.24	6.20
AccD	KMS41_11035	Metabolism	Acetyl-CoA carboxylase β subunit, fatty acid biosynthesis	-1.65	-1.06	-2.39	-2.29	-2.21
PstS	KMS41_11235	Transport	ABC transporter periplasmic binding protein, phosphate transport	7.03	6.56	7.11	7.74	7.21
PstC	KMS41_11240	Transport	ABC transporter permease subunit, phosphate transport	4.07	6.56	7.11	7.74	7.21
PstA	KMS41_11245	Transport	ABC transporter permease subunit, phosphate transport	3.69	3.44	3.92	3.95	3.03
PstB	KMS41_11250	Transport	ABC transporter nucleotide binding protein, phosphate transport	3.95	3.25	4.16	4.20	3.41
PhoU	KMS41_11255	Regulation	Regulatory protein of the PstSCAB phosphate transporter PstB	3.02	2.28	2.86	5.83	5.39

(*continued on next page*)

Table 3 (*continued*)

				Log$_2$ [aminophosphonate/positive control]				
PhoB	KMS41_11260	Transcription regulation	Transcriptional regulator of phosphate uptake genes	5.94	5.24	5.22	5.83	5.39
Uncharacterized	KMS41_12610	Transport	ABC transporter periplasmic binding protein, unknown	2.08	2.58	2.37	3.20	2.47
Uncharacterized	KMS41_13335	Unknown	DUF2147 domain-containing protein, unknown	2.59	1.17	1.70	2.25	1.32
Uncharacterized	KMS41_13505	Unknown	Autotransporter domain-containing protein, unknown	1.42	3.16	1.00	1.57	1.76
Uncharacterized	KMS41_14460	Metabolism	LLM class flavin-dependent oxidoreductase, unknown	-1.41	-1.33	-1.33	-1.47	-3.29
CopC	KMS41_14495	Stress adaptation	Copper resistance protein CopC, binds Cu^{2+}	-1.59	-1.00	-2.09	-2.19	-2.79
Uncharacterized	KMS41_15085	Unknown	Unknown	1.64	1.42	1.63	2.68	1.98
Uncharacterized	KMS41_17085	Transport	ABC transporter periplasmic binding protein, iron transport?	5.56	5.69	5.78	5.51	5.07
Uncharacterized	KMS41_17400	Metabolism	2-Hydroxyacid dehydrogenase, unknown	-3.41	-2.44	-3.41	-3.41	-3.41
PhoA	KMS41_18950	Metabolism	Alkaline phosphatase, adaptation to phosphate starvation	5.85	4.86	6.98	7.24	6.21
Uncharacterized	KMS41_18960	Metabolism	Esterase-like activity of phytase family protein, adaptation to phosphate starvation?	5.01	3.34	6.18	6.62	5.97
Uncharacterized	KMS41_21695	Unknown	Unknown	6.40	2.25	6.82	5.96	4.00
Uncharacterized	KMS41_26600	Unknown	Ferritin-like domain-containing protein, stress adaptation	7.21	1.97	7.49	8.17	6.57
Uncharacterized	KMS41_26670	Unknown	PepSY domain-containing protein, unknown	1.79	1.31	1.87	2.63	2.07

The fact that the proteins of the PstSCAB phosphate uptake complex were enriched in the proteome verified that the bacteria encountered phosphate starvation (Table 3). Moreover, the C-P lyase system involved in the uptake and degradation of aminophosphonates was overproduced in *Ochrobactrum* sp. BTU1 during cultivation with GS, EDTMP, AMPA, IDMP, and EABMP (Table 3). The analysis of the genome sequence revealed that *Ochrobactrum* sp. BTU1 possesses a C-P lyase pathway *phn* operon with a gene order that has been previously described (Hove--Jensen et al., 2014). PhnE and PhnE' are both integral membrane proteins and were, therefore, probably not identified. Furthermore, we could not identify the transcriptional regulator PhnF of phosphonate degradation genes, which is probably less abundant than the structural proteins of the C-P lyase complex. In the case of *Ochrobactrum*, it has been suggested that a second operon encodes the PhnM' paralog of the C-P lyase complex and the DUF1045 protein, which was proposed to be relevant for phosphonate degradation (Huang et al., 2005). The inspection of the genome sequence indeed uncovered the presence of the duf_{1045} and *phnM'* genes (Table 3; Fig. 4). Like in the *Ochrobactrum* strain ATCC 49188, in the isolate *Ochrobactrum* sp. BTU1 the C-P lyase operons are also located on chromosome 1 (Fig. 4) (Chain et al., 2011).

However, in the strain BTU1, the distance between the operons is 263 kbp, and thus, about 83 kbp larger than in the strain ATCC 49188. The PhnM homologs of the strain BTU1 share 62% overall sequence identity. Interestingly, the DUF1045 protein was present in the protein samples obtained from cultures that were supplemented with EDTMP, AMPA, IDMP, and EABMP (Table 3). This indicates that the DUF1045 protein of unknown function might indeed play a role in the degradation of these aminophosphonates. Moreover, in addition to the C-P lyase enzyme complex all components of the sarcosine oxidase complex were overproduced when the strain was cultivated with GS as the single source of phosphate (Table 3). Both enzyme systems are known to be involved in the degradation of aminophosphonates like GS and AMPA (Hove-Jensen et al., 2014; Stosiek et al., 2020). It has been suggested that the methyl moiety of AMPA, which is generated by the C-P lyase enzyme complex from GS, may be transferred to tetrahydrofolate derivatives that are further metabolized in one-carbon metabolism (Hassan-Abdallah et al., 2005). Thus, two enzyme complexes that have been previously shown to be crucial for aminophosphonate degradation were identified in the *Ochrobactrum* isolate sp. BTU1.

Four other enzymes related to phosphate metabolism were also enriched in the proteomes of *Ochrobactrum* sp. BTU1 during cultivation with aminophosphonates. In particular, the polyphosphate kinase Ppk involved in phosphate storage and release, the inorganic pyrophosphatase Ppa, the alkaline phosphatase PhoA and the glycerophosphodiester phosphodiesterase UgpQ were overproduced (Table 3). Ppa and PhoA were proposed to catalyze the last step in the C-P lyase-dependent GS and AMPA degradation pathway (Hove-Jensen et al., 2014). Both enzymes can cleave pyrophosphate to release phosphate. In *E. coli*, the unspecific cytosolic glycerophosphodiester phosphodiesterase UgpQ is synthesized during phosphate starvation (Oshima et al., 2008). It has been suggested that the enzyme allows the utilization of glycerophosphodiesters as a source of phosphate (Oshima et al., 2008). Moreover, the phosphoglucose isomerase Pgi of the glycolytic pathway as well as seven proteins related to transport and nine uncharacterized proteins were more abundant in the cells grown in the presence of the five aminophosphonates. Finally, we also identified seven proteins that were underrepresented in cell during cultivation of the aminophosphonates, among them the γ/τ subunit of the DNA polymerase, the CysQ sulfate assimilation protein, FliJ of the flagellum, the copper homeostasis CopC protein and two uncharacterized proteins (Table 3). It remains to be elucidated why the cellular amount of these proteins were reduced under phosphate.

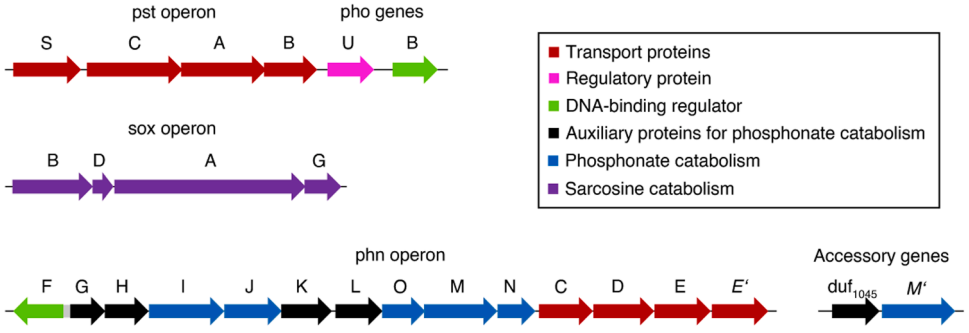

Fig. 4. Organization of the C-P lyase, sarcosine oxidase and phosphate transporter complex genes in *Ochrobactrum* sp. BTU1. The *pstSCAB* operon, the *phoU* and *phoB* genes, the *sox* operon, the *phnGHIJKLOMNCDEE'* gene cluster and the duf_{1045}-*phnM'* operon are located on chromosome 1 (Table 1). The nomenclature for the phn genes encoding the C-P-lyase pathway has been adopted from Hove-Jensen et al. (Hove-Jensen et al., 2014).

4. Discussion

Here, we describe the characterization of the isolate *Ochrobactrum* sp. BTU1 that can break down the aminophosphonates GS, EDTMP, AMPA, IDMP, and EABMP as the only phosphorus source. The latter three substances were included because they are common breakdown products of EDTMP and other aminophosphonates such as DTPMP recently reported for photochemical treatments (Kuhn et al., 2017; Kuhn et al., 2018). Since we also evidenced a similar degradation mechanism for DTPMP under sunlight irradiation releasing AMPA, IDMP and EABMP their potential release in the aquatic environment might still be underestimated (Kuhn et al., 2022). Also, the biodegradation of more complex aminophosphonates such as DTPMP and EDTMP by *Ochrobactrum* sp. was never described into detailed regarding the enzymatic regulations during phosphonate exposure.

Our findings unmistakably affirm that our newly identified isolate falls within the genus *Ochrobactrum*. This is contrary to its initial classification as *Brucella*, as indicated by the NCBI database. Recently, some *Ochrobactrum* strains were mistakenly assumed to be *Brucella*, based on a BLAST Distance Phylogeny approach (a cladistic methodology that uses only genes identified as orthologs using bioinformatic tools) (Hördt et al., 2020). However, care needs to be taken as crucial foundations validating this claim are lacking. Thus, caution is warranted. Certain *Ochrobactrum* strains presumed to be *Brucella* are, in fact, not *Brucellae*. Since the start, *Brucella* and *Ochrobactrum* species have been categorized into distinct genera due to notable distinctions in their phenotypic, genotypic, biological, and epidemiological characteristics. Nevertheless, analyses were conducted to exclude this biosafety level 3 organism, *Brucella*. As above-mentioned, both α-proteobacteria are closely related but we demonstrated that the genome size of our bacteria strain differs significantly from the common genome size characteristic for *Brucella*. The genome of the latter, commonly averages up to 3.4 Mb (Moreno etb al, 2022; Jumas-Bilak et al., 1998). In addition, important virulent factors (i.e. VirB system) as well as important genes for the lipopolysaccharide synthesis and specific resistant genes such as mprF are not present in the genome of our bacteria strain, confirming that the strain does not indeed belong to the genera *Brucella* but to *Ochrobactrum*.

The genus *Ochrobactrum* of which several strains were recently reported shows unique properties to breakdown of different persistent substances such as chlorinated aromatic compounds (Pan et al., 2017), tetrabromobisphenol-A (Liang et al., 2019), dimethylamine (Raj et al., 2019), the insecticide imidacloprid (Erguven and Demirci, 2021), or flame retardant tris(2-ethylhexyl)phosphate (He et al., 2023), to name a few. Also, the potential to reduce chlorate was reported (Chen et al., 2019). Thus, strains of the genus *Ochrobactrum* might be predesignated to degrade and grow on persistent substances utilizing them either as sole sources of carbon, or nitrogen and/or phosphorus or even as energy source.

We have demonstrated that our strain grows on all five aminophosphonate as sole sources of phosphorus. Moreover, the different phosphonate structures supported growth to different extents as reflected by the different doubling times. As *Ochrobactrum* sp. BTU1 grew fastest on the smallest aminophosphonate AMPA and slowest on EDTMP and GS, we assume that the size of chemical structures has major influence not only on the degradation and growth rates but also on the key enzymatic degradation pathway.

The structure of the chosen phosphonates might not only impact the growth rates, but also the choice of the carbon source and its provided amount. High amounts of ammonium acetate has recently been shown to be a limiting growth factor during biodegradation of AMPA by activated sludge (Riedel et al., 2023). Thus, we might also assume carbon limitation being responsible for low biomass yields, especially for EABMP and GS.

Our genome sequencing analysis revealed that the genome of isolate BTU1 contains the *phn* operon and accessory genes as recently reported by Hove-Jensen et al. (2014). In addition, isolate BTU1 contains the *sox* operon required for the oxidation of sarcosine, a metabolite that is generated during GS degradation. However, the genomic analysis does not explain different growth rates observed for the tested aminophosphonates. The combined genomic and proteomic analyses confirm that enzymes belonging to the multi enzyme complex of the C-P lyase are involved in the degradation of aminophosphonates but most likely promoting different degradation pathways for GS on the one hand, and for EDTMP, AMPA, IDMP and EABMP, on the other hand.

In recent literature, two different degradation pathways for GS are described, i.e., the AMPA pathway and the sarcosine pathway (Rossi et al., 2021; Hertel et al., 2021; Hove-Jensen et al., 2014). In the former pathway, glyphosate oxidase mediates the initial cleavage of GS at the C-N bond resulting in formation of AMPA and glyoxylate. According to Ermakova et al. (2017) the enzymatic mechanism of *Ochrobactrum anthropi* to degrade AMPA released from GS is still uncertain. There are some hints reported by Gard et al. (1997) that AMPA undergoes either methylation or acetylation while Sviridov et al. (2012) proposed transamination of AMPA without detailed knowledge of the cleavage mechanism.

In the sarcosine pathway, however, the C-P lyase mediates the initial cleavage at the C-P bond resulting in formation of sarcosine and P_i. Overexpression of all four sarcosine oxidase subunits occurred only when isolate BTU1 was exposed to GS. Therefore, we can hypothesise that GS degradation is promoted by C-P lyase via the sarcosine pathway. In contrast, overproduction of Duf_{1045}, a member of two-histidine phosphodiesterase, occurred for all aminophosphonates excluding GS. Thus, Duf_{1045} seems to be exclusively involved in the degradation of EDTMP, AMPA, IDMP and EABMP. Differential overproduction of key enzymes such as sarcosine oxidase and Duf_{1045}, different degradation and growth rates may indicate that the initial cleavage of GS and the other four aminophosphonates is different. Cleavage of the C-P bond must occur as initial stage mediating the sarcosine pathway for GS degradation. Cleavage of the C-N bond as initial stage might exclusively occur for the other four aminophosphonates. For example, the detection of the metabolite ethylenediaminetri(methylenephosphonic acid) (*m/z* 341) in cell free media underlines the initial cleavage of EDTMP at the C-N bond. It is conceivable that the resulting intermediate methylphosphonate is then utilized as initial substrate to start the biosynthesis of ribose-1-phosphonate mediated by C-P lyase (Kamat and Raushel, 2013; Sviridov et al., 2012). Thus, different degradation pathways mediated by similar enzymes are suggested for GS and the other four aminophosphonates. Recently, it has been proposed that pathways for the degradation of GS may vary among different *Ochrobactrum* strains (Chen et al., 2022; Rossi et al., 2021; Ermakova et al., 2017; Hadi et al., 2013; Sviridov et al., 2012). The degradation of more complex aminophosphonates such as EDTMP was not demonstrated so far.

Interestingly, Sviridov et al. (2012) demonstrated for strain *Ochrobactrum anthropi* GPK3 the presence of a C-P lyase system I and C-P lyase system II. The former C-P system utilizes only methylphosphonate and the latter was assigned as glyphosate-specific C-P lyase leading to formation of sarcosine (Stosiek et al., 2020). However, our genomic data did not confirm the presence of alternative genes encoding two different C-P lyase systems as in strain *Ochrobactrum anthropi* GPK 3. Therefore, it is unlikely that an alternative C-P lyase system for the degradation of EDTMP, AMPA, IDMP and EABMP exists in *Ochrobactrum* sp. BTU1. However, the expression of proteins like Duf_{1045} and other proteins of unknown function points to a yet unknown pathway that could be involved in degradation of more complex aminophosphonates.

Independent of how GS and the other synthetic aminophosphonates are degraded, it is very likely that their uptakes are under direct control

of the *pst* operon regulating the Pi supply. We performed the degradation tests under strict phosphorus starving conditions. It is well known that concentrations below 4 μM of inorganic phosphate the Pho regulon is encoded (Stosiek et al., 2020). Our proteomic analyses confirmed similar overexpression for all five aminophosphonates, especially of PhoB which induces the transcription of the Pho regulon. The overexpression of *pstSCAB-phoU* genes confirms the increased regulation of transport and metabolism of phosphonic acids from the environment (Metcalf and Wanner, 1993). In consequence, up-regulation of the Pho regulon was expectable and confirmed.

Despite different enzymatic cleavage of GS and the other four aminophosphonates, one has to bear in mind that GS directly inhibits the precursor of de novo synthesis of the aromatic amino acids phenylalanine, tyrosine and tryptophan as well as of the vitamins folic acid and menaquinone (Hertel et al., 2021). Similar effects of other aminophosphonates such as AMPA can be excluded because only GS can replace phosphoenolpyruvate (PEP) in the active site of the 5-enolpyruvyl-shikimate-3-phosphate (EPSP) synthase (Hertel et al., 2021). Therefore, increased toxicity was recently assumed for GS as compared to AMPA (Rossi et al., 2021). It might be speculated that EDTMP, AMPA, IDMP and EABMP show lower toxicity than GS due to no direct affecting EPSP. However, we must also assume negative effects of the metal chelator EDTMP on the general physiology of the bacteria resulting in similar reduced growth rates as GS.

Finally, our new isolate *Ochrobactrum* sp. BTU1 could be applied as platform for more detailed studies including extensive expression studies and enzyme assays as well as overexpression of candidate genes and construction of knockout mutants. The high abundance of Pst phosphate transporter indicated phosphate starvation in *Ochrobactrum* sp. BTU1 during degradation of all five aminophosphonates. The inhibited expression of *phn* genes in the presence of phosphate could explain the observed long lifetime of aminophosphonates in the environment. This limitation should be considered when monitoring aminophosphonate in the environment and when designing wastewater treatment plants for their better removal.

5. Conclusion

We characterised and investigated bacteria strain *Ochrobactrum* sp. BTU1. The initial genomic analysis revealed that the strain belongs to the genera of *Brucella* or *Ochrobactrum*. In silico detection of AMR genes (i.e., absence of VirB system), however, confirmed that our strain belongs to the genera of *Ochrobactrum*. Antibiotic susceptibility tests showed that *Ochrobactrum* sp. BTU1 is only resistant to sulfonamide. Biodegradation tests of selected aminophosphonates indicated different duration of the lag phases which seem to depend on the phosphonate chemical structure. The shortest lag phase was determined for AMPA while EDTMP resulted in the longest lag phase. The growth rates were highest for AMPA and lowest for EDTMP and GS. Results of the proteomic analyses confirmed that *Ochrobactrum* sp. BTU1 possess a C-P lyase located on chromosome 1. However, only for GS all four sarcosine oxidase subunits were found to be overproduced. The sarcosine pathway mediates the initial cleavage at the C-P bond, which we can only confirm for GS degradation. In contrast, Duf_{1045} seems to be exclusively involved in the degradation of EDTMP, AMPA, IDMP and EABMP. Results of our LC/MS analysis of the mother compounds confirmed the presence of *m/z* 341 in the cell free medium for EDTMP. This cleavage product can only be release if the initial cleavage occurs at the C-N. Therefore, we propose different initial cleavage mechanism for GS and the other four synthetic aminophosphonates with a similar subset of enzymes involved.

Author Statement

The authors confirm that there were no commercial or financial affiliations that could be interpreted as a possible conflict of interest during the course of the research.

CRediT authorship contribution statement

Martienssen Marion: Writing – review & editing. **Mardoukhi Mohammad Saba Yousef:** Investigation. **Noack Laura Emelie:** Investigation. **Holzer Katharina:** Data curation, Investigation, Software, Validation, Writing – review & editing. **Hoelzle Ludwig E.:** Data curation, Investigation, Software, Validation. **Hertel Robert:** Data curation, Investigation, Supervision. **Commichau Fabian M.:** Data curation, Investigation, Supervision, Writing – original draft, Writing – review & editing. **Benndorf Dirk:** Data curation, Investigation, Supervision, Writing – original draft, Writing – review & editing. **Riedel Ramona:** Conceptualization, Investigation, Methodology, Project administration, Supervision, Validation, Visualization, Writing – original draft, Writing – review & editing, Data curation.

Data Availability

The genomic data are available at NCBI.

Acknowledgments

The authors thank "Zschimmer & Schwarz" for providing several phosphonate compounds. The authors are grateful to Brigitte Herrmann, Kathrin Krahl and Kai Buder for technical support. This work was supported by the Deutsche Forschungsgemeinschaft (CO 1139/3–1 to F.M. C.). The authors are grateful to Isaac Mbir Bryant for critical improving and revising the manuscript.

Appendix A. Supporting information

Supplementary data associated with this article can be found in the online version at doi:10.1016/j.micres.2024.127600.

References

Achari, A., Somer, D.O., Champness, J.N., Bryant, P.K., Rosemond, J., Stammers, D.K., 1997. Crystal structure of the anti-bacterial sulfonamide drug target dihydropteroate synthase. Nat. Struc. Biol. 4 (6), 490–497. https://doi.org/10.1038/nsb0697-490.

Armbruster, D., Rott, E., Minke, R., Happel, O., 2020. Trace-level determination of phosphonates in liquid and solid phase of wastewater and environmental samples by IC-ESI-MS/MS. Anal. Bioanal. Chem. 412, 4807–4825. https://doi.org/10.1007/s00216-019-02159-5.

Bankevich, A., Nurk, S., Antipov, D., Gurevich, A.A., Dvorkin, M., Kulikov, A.S., Lesin, V. M., Nikolenko, S.I., Pham, S., Prjibelski, A.D., Pyshkin, A.V., Sirotkin, A.V., Vyahhi, N., Tesler, G., Alekseyev, M.A., Pevzner, P.A., 2012. SPAdes: a new genome assembly algorithm and its applications to single-cell sequencing. J. Comput. Biol. 19 (5), 455–477. https://doi.org/10.1089/cmb.2012.0021.

Boschiroli, M.L., Ouahrani-Bettache, S., Foulongne, V., Michaux-Charachon, S., Bourg, G., Allardet-Servent, A., Cazevieille, C., Liautard, J.P., Ramuz, M., O'Callaghan, D., 2002. The *Brucella suis virB* operon is induced intracellularly in macrophages. Proc. Natl. Acad. Sci. Usa. 99 (3), 1544–1549. https://doi.org/10.1073/pnas.032514299.

Chain, P.S., Lang, D.M., Comerci, D.J., Malfatti, S.A., Vergez, L.M., Shin, M., Ugalde, R. A., Garcia, E., Tomalsky, M.E., 2011. Genome of *Ochrobactrum anthropi* ATCC 49188 T, a versatile opportunistic pathogen and symbiont of several eukaryotic hosts. J. Bacteriol. 193 (16), 4274–4275. https://doi.org/10.1128/JB.05335-11.

Chen, H.W., Xu, M., Ma, X.W., Tong, Z.H., Liu, D.F., 2019. Isolation and characterization of a chlorate-reducing bacterium *Ochrobactrum antrophi* XM-1. J. Hazard. Mat. 380, 120873 https://doi.org/10.1016/j.jhazmat.2019.120873.

Chen, Y., Chen, W.J., Huang, Y., Li, J., Zhong, J., Zhang, W., Zou, Y., Mishra, S., Bhatt, P., Chen, S., 2022. Insights into the microbial degradation and resistance mechanisms of glyphosate. Environ. Res. 215 (Pt 1), 114153 https://doi.org/10.1016/j.envres.2022.114153.

Erguven, G.O., Demirci, U., 2021. Using *Ochrobactrum thiophenivorans* and *Sphingomonas melonis* for bioremediation of imidacloprid. Environ. Technol. Innov.. 21, 101236 https://doi.org/10.1016/j.eti.2020.101236.

Ermakova, I.T., Shushkova, T.V., Sviridov, A.V., Zelenkova, N.F., Vinokurova, N.G., Baskunov, B.P., Leontievsky, A.A., 2017. Organophosphonates utilization by soil strains of *Ochrobactrum anthropi* and *Achromobacter* sp. Arch. Microbiol.. 199, 665–675. https://doi.org/10.1007/s00203-017-1343-8.

Frederikson, N.J., Hermansson, M., Wilén, B.M., 2013. The choice of PCR primers has great impact on assessments of bacterial community diversity and dynamics in a wastewater treatment plant. PLoS One 8 (10), e76431. https://doi.org/10.1371/journal.pone.0076431.

Gard, J.K., Feng, P.C.C., Hutton, W.C., 1997. Nuclear magnetic resonance timecourse studies of glyphosate metabolism by microbial isolates. Xenobiotica 27 (7), 633–644. https://doi.org/10.1080/00498259720235.

Grandcoin, A., Piel, S., Baurès, E., 2017. AminoMethylPhosphonic acid (AMPA) in natural waters: its source, behavior and environmental fate. Water Res 117, 187–197. https://doi.org/10.1016/j.waters.2017.03.055.

Gurevich, A., Saveliev, V., Vyahhi, N., Tesler, G., 2013. QUAST: quality assessment tool for genome assemblies, 1072-1017 : Bioinforma. (Oxf., Engl.) 28 (8). https://doi.org/10.1093/bioinformatics/btt086.

Hadi, F., Mousavi, A., Akbari, N.K., Ghaderi, T.H., Hatef, S.A., 2013. New bacterial strain of the genus *Ochrobactrum* with glyphosate-degrading activity. J. Environ. Sci. Health B 48, 208–213. https://doi.org/10.1080/03601234.2013.730319.

Hassan-Abdallah, A., Zhao, G., Eschenbrenner, M., Chen, Z.W., Mathews, F.S., Jorns, M. S., 2005. Cloning, expression and crystallization of heterotetrameric sarcosine oxidase from *Pseudomonas maltophilia*. Protein Expr. Purif. 43 (1), 33–43. https://doi.org/10.1016/j.pep.2005.03.023.

He, J., Wang, Z., Zhen, F., Wang, Z., Song, Z., Chen, J., Hrynsphan, D., Tatsiana, S., 2023. Mechanisms of flame retardant tris (2-ethylhexyl) phosphate biodegradation via novel bacterial strain *Ochrobactrum tritici* WX3-8. Chemosphere 311 (Pt 2), 137071. https://doi.org/10.1016/j.chemosphere.2022.137071.

Hertel, R., Gibhardt, J., Martienssen, M., Kuhn, R., Commichau, F.M., 2021. Molecular mechanisms underlying glyphosate resistance in bacteria. Environ. Microbiol. 23 (6), 2891–2905. https://doi.org/10.1111/1462-2920.15534.

Hertel, R., Schöne, K., Mittelstädt, C., Meißner, J., Zschoche, N., Collignon, M., Kohler, C., Friedrich, I., Schneider, D., Hoppert, M., Kuhn, R., Schwedt, I., Scholz, P., Poehlein, A., Martienssen, M., Ischebeck, T., Daniel, R., Commichau, F.M., 2022. Characterization of glyphosate-resistant *Burkholderia anthina* and *Burkholderia cenocepacia* isolates from a commercial Roundup® solution. Environ. Microbiol. Rep.. 14 (1), 70–84. https://doi.org/10.1111/1758-2229.13022.

Heyer, R., Schallert, K., Büdel, A., Zoun, R., Dorl, S., Behne, A., Kohrs, F., Püttker, S., Siewert, C., Muth, T., Saake, G., Reichl, U., Benndorf, D., 2019. A robust and universal metaproteomics workflow for research studies and routine diagnostics within 24h using phenol extraction, FASP digest, and the MetaProteome Analyzer. Front. Microbiol. 10, 1883 https://doi.org/10.3389/fmicb.2019.01883.

Holzer, K., Hoelzle, L.E., Wareth, G., 2023. Genetic comparison of Brucella spp. And Ochrobactrum spp. Erroneously included into the Brucella confirms separate genera. Ger. J. Vet. Res. 3 (1), 31–37. https://doi.org/10.51585/gjvr.2023.1.0050.

Hördt, A., López, M.G., Meier-Kolthoff, J.P., Schleuning, M., Weinhold, L.M., Tindall, B. J., Gronow, S., Kyrpides, N.C., Woyke, T., Göker, M., 2020. Analysis of 1000+ type-strain genomes substantially improves taxonomic classification of *Alphaproteobacteria*. Front. Microbiol. 11, 468 https://doi.org/10.3389/fmicb.2020.00468.

Horsman, G.P., Zechel, D.L., 2017. Phosphonate biochemistry. Chem. Rev. 117 (8), 5704–5783. https://doi.org/10.1021/acs.chemrev.6b00536.

Hove-Jensen, B., Zechel, D., Jochimsen, B., 2014. Utilization of glyphosate as phosphate source: biochemistry and genetics of bacterial carbon-phosphorus lyase. Microbiol. Mol. Biol. Rev. 78 (1), 176–197. https://doi.org/10.1128/MMBR.00040-13.

Hsieh, Y.J., Wanner, B.L., 2010. Global regulation by the seven-component P_i signalling system. Curr. Opin. Microbiol. 13 (2), 198–203. https://doi.org/10.1016/j.mib.2010.01.014.

Huang, J., Su, Z., Xu, Y., 2005. The evolution of microbial phosphonate degradation pathways. J. Mol. Evol. 61 (5), 682–690. https://doi.org/10.1007/s00239-004-0349-4.

Huntscha, S., Stravs, M.A., Bühlmann, A., Ahrens, C.H., Frey, J.E., Pomati, F., Hollender, J., Buerge, I.J., Balmer, M.E., Poiger, T., 2018. Seasonal dynamics of glyphosate and AMPA in lake Greifensee: rapid microbial degradation in the epilimnion during summer. Environ. Sci. Technol. 52 (8), 4641–4649. https://doi.org/10.1021/acs.est.8b00314.

Jaworska, J., Van Genderen-Takken, H., Hanstveit, A., van de Plassche, E., Feijtel, T., 2002. Environmental risk assessment of phosphonates, used in domestic laundry and cleaning agents in the Netherlands. Chemosphere 47 (6), 655–665. https://doi.org/10.1016/S0045-6535(01)00328-9.

Jumas-Bilak, E., Michaux-Charachon, S., Bourg, G., O'Callaghan, D., Ramuz, M., 1998. Differences in chromosome number and genome rearrangements in the genus Brucella. Mol. Microbiol. 27 (1), 99–106. https://doi.org/10.1046/j.1365-2958.1998.00661.x.

Kamat, S.S., Raushel, F.M., 2013. The enzymatic conversion of phosphonates to phosphate by bacteria. Curr. Opin. Chem. Biol. 17 (4), 589–596. https://doi.org/10.1016/j.cbpa.2013.06.006.

Ke, Y., Wang, Y., Li, W., Chen, Z., 2015. Type IV secretion system of *Brucella* spp. and its effectors. Front. Cell. Infect. Microbiol. 5, 72. https://doi.org/10.3389/fcimb.2015.00072.

Knepper, T.P., 2003. Synthetic chelating agents and compounds exhibiting complexing properties in the aquatic environment. Trends Anal. Chem. 22, 707–724. https://doi.org/10.1016/S0165-9936(03)01008-2.

Küchler, J., Willenbücher, K., Reiß, E., Nuß, L., Conrady, M., Ramm, P., Schimpf, U., Reichl, U., Szewzyk, U., Benndorf, D., 2023. Degradation kinetics of lignocellulolytic enzymes in a biogas reactor using quantitative mass spectrometry. Fermentation 9 (1), 67. https://doi.org/10.3390/fermentation9010067.

Kuhn, R., Tóth, E., Geppert, H., Fischer, T., Liebsch, S., Martienssen, M., 2017. Identification of the complete photodegradation pathway of ethylenediaminetetra (methylenephosphonic acid) in aquatic solution. Clean. Soil Air Water 45 (5), 1–8. https://doi.org/10.1002/clen.201500774.

Kuhn, R., Jensch, R., Bryant, I.M., Fischer, T., Liebsch, S., Martienssen, M., 2018. The influence of selected bivalent metal ions on the photolysis of diethylenetriamine penta(methylenephosphonic acid). Chemosphere 210, 726–733. https://doi.org/10.1016/j.chemosphere.2018.07.033.

Kuhn, R., Jensch, R., Bryant, I.M., Fischer, T., Liebsch, S., Martienssen, M., 2020. Rapid sample clean-up procedure for aminophosphonate determination by LC/MS analysis. Talanta 208, 120454. https://doi.org/10.1016/j.talanta.2019.120454.

Kuhn, R., Jensch, R., Fischer, T., Keuler, K., Bryant, I.M., Martienssen, M., 2022. Sunlight degradation of the aminophosphonates diethylenetriamine penta-(methylenephosphonic acid). Solar 2 (2), 141–157. https://doi.org/10.3390/solar2020009.

Lesueur, C., Pfeffer, M., Fuerhacker, M., 2005. Photodegradation of phosphonates in water. Chemosphere 59 (5), 685–691. https://doi.org/10.1016/j.chemosphere.2004.10.049.

Li, J., Liu, H., Liu, Z., Zhang, X., Blake, R.E., Huang, Z., Cai, M., Wang, F., Yu, C., 2023. Transformation mechanism of methylphosphonate to methane by Burkholdria sp: Insight from multi-labeled water isotope probing and transcriptomic. Environ. Res. 218, 114970 https://doi.org/10.1016/j.envres.2022.114970.

Liang, Z., Li, G., Mai, B., Ma, H., An, T., 2019. Application of a novel gene encoding bromophenol dehydrogenase from *Ochrobactrum* sp. Z in TBBPA degradation. Chemosphere 217, 507–515. https://doi.org/10.1016/j.chemosphere.2018.11.004.

Liu, B., Zheng, D., Jin, Q., Chen, L., Yabng, J., 2019. VFDB 2019: a comparative pathogenomic platform with an interactive web interface. Nucleic Acids Res 47 (D1), 687–692. https://doi.org/10.1093/nar/gky1080.

McSorley, F.R., Wyatt, P.B., Martinez, A., DeLong, E.F., Hoven-Jensen, B.M., Zechel, D.L., 2012. PhnY and PhnZ comprise a new oxidative pathway for enzymatic cleavage of a carbon-phosphorus bond. J. Am. Chem. Soc. 134 (20), 8364–8367. https://doi.org/10.1021/ja302072f.

Metcalf, W.W., Wanner, B.L., 1993. Evidence for a fourteen-gene, *phnC* to *phnP* locus for phosphonate metabolism in *Escherichia coli*. Gene 129 (1), 27–32. https://doi.org/10.1016/0378-1119(93)90692-v.

Moreno, E., Blasco, J.M., Letesson, J.J., Gorvel, J.P., Moriyón, I., 2022. Pathogenicity and its implications in taxonomy: the *Brucella* and *Ochrobactrum* case. Pathogens 11 (3), 377. https://doi.org/10.3390/pathogens11030377.

Njeru, J., Wareth, G., Melzer, F., Henning, K., Pletz, M.W., Heller, R., Neubauer, H., 2016. Systematic review of brucellosis in Kenya: Disease frequency in humans and animals and risk factors for human infection. BMC Public Health 16 (1), 853. https://doi.org/10.1186/s12889-016-3532-9.

Nowack, B., 1998. The behavior of phosphonates in wastewater treatment plants of Switzerland. Water Res 32 (4), 1271–1279. https://doi.org/10.1016/S0043-1354(97)00338-2.

Nowack, B., 2003. Environmental chemistry of phosphonates. Water Res 37 (1), 2533–2546. https://doi.org/10.1016/S0043-1354(03)00079-4.

Obojska, A., Lejczak, B., Kubrak, M., 1999. Degradation of phosphonates by *Streptomycete* isolates. Appl. Microbiol. Biotechnol. 51 (6), 872–876. https://doi.org/10.1007/s002530051476.

Oshima, N., Yamashita, S., Takahashi, N., Kuroishi, C., Shiro, Y., Takio, K., 2008. *Escherichia coli* cytosolic glycerophosphodiester phosphodiesterase (UgpQ) requires Mg^{2+}, Co^{2+}, or Mn^{2+} for its enzyme activity. J. Bacteriol. 190 (4), 1219–1223. https://doi.org/10.1128/JB.01223-07.

Pallitsch, K., Zechel, D.L., 2023. The functional importance of bacterial oxidative phosphonate pathways. Biochem. Soc. Trans. 51, 487–499. https://doi.org/10.1042/BST20220479.

Pan, X., Xu, T., Xu, H., Fang, H., Yu, Y., 2017. Characterization and genome functional analysis of the DDT-degrading bacterium *Ochrobactrum* sp. DDT-2. Sci. Tot. Environ. 592, 593–599. https://doi.org/10.1016/j.scitotenv.2017.03.052.

Pfennig, N., Trüper, H.G., 1981. Isolation of members of the Families *Chromatiaceae* and *Chlorobiaceae*. In: Starr, M.P., Stolp, H., Trüper, H.G., Balows, A., Schegel, H.G. (Eds.), The Prokaryotes, Vol. 1. Springer, Berlin, Heidelberg, pp. 279–289. https://doi.org/10.1007/978-3-662-13187-9_16.

Raj, I., Bansiwal, A., Vaidya, A.N., 2019. Kinetic evaluation for rapid degradation of dimethylamine enriched with *Agromyces* and *Ochrobactrum* sp. J. Environ. Manag.. 245, 322–329. https://doi.org/10.1016/j.jenvman.2019.05.074.

Riedel, R., Krahl, K., Buder, K., Böllmann, J., Braun, B., Martienssen, M., 2023. Novel standard biodegradation test for synthetic phosphonates. J. Microbiol. Methods 212, 106793. https://doi.org/10.1016/j.mimet.2023.106793.

Rossi, F., Carles, L., Donnadieu, F., Batisson, I., Artigas, J., 2021. Glyphosate-degrading behavior of five bacterial strains isolated from stream biofilms. J. Hazard. Mat. 420, 126651 https://doi.org/10.1016/j.jhazmat.2021.126651.

Rott, E., Steinmetz, H., Metzger, J.W., 2018. Organophosphonates: a review on environmental relevance, biodegradability and removal in wastewater treatment plants. Sci. Total Environ. 615, 1176–1191. https://doi.org/10.1016/j.scitotenv.2017.09.223.

Ruffolo, F., Dinhof, T., Murray, L., Zangelmi, E., Chin, J.P., Pallitsch, K., Peracchi, A., 2023. The microbial degradation of natural and antropgenic phosphonates. Molecules 28, 6863. https://doi.org/10.3390/molecules28196863.

Schmidt, C.K., Raue, B., Brauch, H.J., Sacher, F., 2014. Trace-level analysis of phosphonates in environmental waters by ion chromatography and inductively coupled plasma mass spectrometry. Intern. J. Environ. Anal. Chem. 94 (4), 385–398. https://doi.org/10.1080/03067319.2013.831410.

Stosiek, N., Talma, M., Klimek-Ochab, M., 2020. Carbon-phosphorus lyase – the state of the art. Appl. Biochem. Biotechnol. 190 (4), 1525–1552. https://doi.org/10.1007/s12010-019-03161-4.

Studnik, H., Liebsch, S., Forlani, G., Wieczorek, D., Kafarski, P., Lipok, J., 2015. Amino polyphosphonates – chemical features and practical uses, environmental durability and biodegradation. N. Biotechnol. 32, 1–6. https://doi.org/10.1016/j.nbt.2014.06.007.

Sviridov, A.V., Shushkova, T.V., Zelenkova, N.F., Vinokurova, N.G., Morgunov, I.G., Ermakova, I.T., Leontievsky, A.A., 2012. Distribution of glyphosate and methylphosphonate catabolism in soil bacteria *Ochrobactrum anthropic* and *Achromobacter* sp. Appl. Microbiol. Biotechnol. 93 (2), 787–796. https://doi.org/10.1007/s00253-011-3485-y.

Ternan, N.G., McGrath, J.W., Quinn, J.P., 1998. Phosphoenolpyruvate phosphomutase activity in an L-phosphono alanine-mineralizing strain of *Burkholdria cepacia*. Appl. Environ. Microbiol.. 64 (6), 2291–2294. https://doi.org/10.1128/aem.64.6.2291-2294.1998.

Villarreal-Chiu, J.F., Quinn, J.P., McGrath, J.W., 2012. The genes and enzymes of phosphonate metabolism by bacteria, and their distribution in the marine environment. Front. Microbiol. 3, 1–13. https://doi.org/10.3389/fmicb.2012.00019.

Wang, S., Sun, S., Shan, C., Pan, B., 2019. Analysis of trace phosphonates in authentic water samples by pre-methylation and LC/Orbitrap MS/MS. Water Res 161, 78–88. https://doi.org/10.1016/j.watres.2019.05.099.

Wiśniewski, J.R., Zougman, A., Nagaraj, N., Mann, M., 2009. Universal sample preparation method for proteome analysis. Nat. Methods 6 (5), 359–362. https://doi.org/10.1038/nmeth.1322.

Zhang, Q., Van der Donk, W.A., 2013. Answers to the carbon-phosphorus lyase conundrum. Chembiochem 13 (5), 627–629. https://doi.org/10.1002/cbic.201200020.